



*Supplement of*

**Meteorology impact on  $PM_{2.5}$  change over a receptor region in the regional transport of air pollutants: observational study of recent emission reductions in central China**

**Xiaoyun Sun et al.**

*Correspondence to:* Tianliang Zhao (tlzhao@nuist.edu.cn) and Yongqing Bai (baiyq2007@126.com)

The copyright of individual parts of the supplement might differ from the article licence.

**Table S1** Linear correlation coefficients of the baseline components ( $PM_{2.5BL}$ ) of daily  $PM_{2.5}$  concentrations respectively with the baseline components of air temperature ( $T_{BL}$ ), relative humidity ( $RH_{BL}$ ), wind speed ( $WS_{BL}$ ), sea level pressure ( $SLP_{BL}$ ) and precipitation ( $Pre_{BL}$ ) in 14 sites over the THB.

Sites	Linear correlation coefficients with $PM_{2.5BL}$				
	$T_{BL}$	$RH_{BL}$	$WS_{BL}$	$SLP_{BL}$	$Pre_{BL}$
JZ	-0.81**	-0.26**	-0.43**	0.79**	-0.50**
XN	-0.82**	-0.04	-0.42**	0.79**	-0.37**
XY	-0.88**	-0.25**	-0.24**	0.85**	-0.41**
JM	-0.86**	-0.38**	0.11**	0.83**	-0.58**
YC	-0.84**	-0.29**	-0.11**	0.79**	-0.57**
SZ	-0.84**	-0.20**	0.00	0.82**	-0.43**
WH	-0.85**	-0.06*	-0.10**	0.81**	-0.37**
EZ	-0.79**	-0.04	-0.23**	0.75**	-0.25**
HG	-0.81**	-0.14**	0.08**	0.75**	-0.28**
HS	-0.70**	-0.05*	-0.42**	0.67**	-0.57**
CS	-0.83**	-0.20**	-0.15**	0.84**	-0.43**
YY	-0.84**	-0.26**	-0.24**	0.85**	-0.41**
XG	-0.82**	-0.13**	-0.07**	0.80**	-0.39**
CD	-0.81**	-0.33**	-0.33**	0.81**	-0.55**

\*\* Passing the confidence level of 99 %, \* Passing the confidence level of 95 %.

**Table S2** Linear correlation coefficients of the baseline components ( $SO_{2BL}$ ) of daily  $SO_2$  concentrations respectively with the baseline components of air temperature ( $T_{BL}$ ), relative humidity ( $RH_{BL}$ ), wind speed ( $WS_{BL}$ ), sea level pressure ( $SLP_{BL}$ ) and precipitation ( $Pre_{BL}$ ) in 14 sites over the THB.

Sites	Linear correlation coefficients with $SO_{2BL}$				
	$T_{BL}$	$RH_{BL}$	$WS_{BL}$	$SLP_{BL}$	$Pre_{BL}$
JZ	-0.61**	-0.27*	-0.27**	0.61**	-0.30**
XN	-0.16**	0.02	-0.21**	0.19**	-0.12**
XY	-0.73**	-0.44**	-0.12**	0.76**	-0.22**
JM	-0.54**	-0.34**	0.19**	0.50**	-0.25**
YC	-0.50**	-0.08**	0.03	0.48**	-0.25**
SZ	-0.55**	-0.17**	0.18**	0.56**	-0.23**
WH	-0.51**	-0.05*	-0.09**	0.51**	-0.26**
EZ	-0.39**	-0.30**	-0.42**	0.38**	-0.02
HG	-0.23**	-0.30**	0.03	0.28**	-0.15**
HS	-0.38**	-0.22**	-0.14**	0.33**	-0.39**
CS	-0.34**	0.08**	0.05*	0.31**	-0.06**
YY	-0.07**	0.00	0.23**	0.09**	0.07**
XG	-0.61**	-0.14*	0.13**	0.61**	-0.26**
CD	-0.23**	-0.07*	0.21**	0.26**	-0.16**

\*\* Passing the confidence level of 99 %, \* Passing the confidence level of 95 %.

**Table S3** Linear correlation coefficients of the baseline components ( $\text{NO}_{2\text{BL}}$ ) of daily  $\text{NO}_2$  concentrations respectively with the baseline components of air temperature ( $T_{\text{BL}}$ ), relative humidity ( $\text{RH}_{\text{BL}}$ ), wind speed ( $\text{WS}_{\text{BL}}$ ), sea level pressure ( $\text{SLP}_{\text{BL}}$ ) and precipitation ( $\text{Pre}_{\text{BL}}$ ) in 14 sites over the THB.

Sites	Linear correlation coefficients with $\text{NO}_{2\text{BL}}$				
	$T_{\text{BL}}$	$\text{RH}_{\text{BL}}$	$\text{WS}_{\text{BL}}$	$\text{SLP}_{\text{BL}}$	$\text{Pre}_{\text{BL}}$
JZ	-0.79**	-0.38**	-0.63**	0.85**	-0.55**
XN	-0.80**	-0.16**	-0.29**	0.85**	-0.54**
XY	-0.81**	-0.38**	-0.41**	0.88**	-0.37**
JM	-0.75**	-0.46**	0.21**	0.79**	-0.58**
YC	-0.76**	-0.29**	-0.17**	0.78**	-0.50**
SZ	-0.87**	-0.40**	-0.21**	0.90**	-0.63**
WH	-0.77**	-0.13**	-0.30**	0.78**	-0.35**
EZ	-0.82**	0.01	0.17**	0.84**	-0.44**
HG	-0.80**	-0.15**	-0.07**	0.83**	-0.39**
HS	-0.81**	0.04	-0.36**	0.80**	-0.68**
CS	-0.80**	-0.16**	-0.21**	0.83**	-0.38**
YY	-0.76**	-0.39**	-0.51**	0.78**	-0.41**
XG	-0.85**	-0.29**	-0.21**	0.85**	-0.37**
CD	-0.76**	-0.34**	-0.21**	0.82**	-0.53**

\*\* Passing the confidence level of 99 %, \* Passing the confidence level of 95 %.

**Table S4** The linear trends  $k_{LT}$  of long-term PM<sub>2.5</sub>, SO<sub>2</sub> and NO<sub>2</sub> and the linear trends  $k_{emiss}$  of emission-related long-term components (Unit: 10<sup>-2</sup> μg m<sup>-3</sup> d<sup>-1</sup>), as well as the ratio of  $k_{LT}$  and  $k_{emiss}$  in the THB.

Sites	PM <sub>2.5</sub>			SO <sub>2</sub>			NO <sub>2</sub>		
	$k_{LT}$	$k_{emiss}$	$\frac{k_{LT}}{k_{emiss}}$	$k_{LT}$	$k_{emiss}$	$\frac{k_{LT}}{k_{emiss}}$	$k_{LT}$	$k_{emiss}$	$\frac{k_{LT}}{k_{emiss}}$
JZ	-1.51	-1.62	0.93	-0.98	-0.92	1.06	-0.23	-0.18	1.28
XN	-1.12	-1.06	1.06	-0.48	-0.45	1.06	0.33	0.29	1.14
XY	-0.18	-0.07	2.57	-0.09	-0.09	1.00	0.12	0.19	0.63
JM	-0.62	-0.57	1.09	-0.82	-0.82	1.00	-0.07	-0.08	0.88
YC	-1.00	-1.20	0.83	-0.66	-0.56	1.18	-0.33	-0.29	1.14
SZ	-1.35	-1.22	1.11	-0.49	-0.42	1.17	-0.10	-0.13	0.77
WH	-1.30	-1.40	0.93	-0.63	-0.65	0.97	-0.46	-0.53	0.87
EZ	-1.59	-0.99	1.61	-0.70	-0.44	1.59	0.18	0.06	3.00
HG	-1.07	-1.08	0.99	-0.29	-0.28	1.04	-0.22	-0.20	1.10
HS	-1.69	-1.49	1.13	-0.38	-0.32	1.18	0.31	0.30	1.03
CS	-0.84	-1.03	0.82	-0.67	-0.66	1.02	-0.39	-0.41	0.95
YY	-0.61	-0.68	0.90	-1.17	-0.99	1.18	0.07	-0.09	-0.78
XG	-1.16	-1.15	1.01	-0.27	-0.21	1.28	-0.16	-0.16	1.00
CD	-0.66	-0.83	0.80	-0.90	-0.72	1.25	-0.34	-0.27	1.26

**Table S5** The linear trends  $k_{LT}$  of long-term PM<sub>2.5</sub> and the linear trends  $k_{emiss}$  of emission-related long-term components, as well as the contribution rates  $Con_{met}$  of meteorology calculated with Eq.(10) in the THB.

Sites	$k_{LT}$ ( $10^{-2} \mu\text{g m}^{-3} \text{d}^{-1}$ )	$k_{emiss}$ ( $10^{-2} \mu\text{g m}^{-3} \text{d}^{-1}$ )	$Con_{met}$ (%)
XY	-0.18	-0.07	61.92
JM	-0.62	-0.07	7.81
JZ	-1.51	-1.62	-6.91
SZ	-1.35	-1.22	9.95
XG	-1.16	-1.15	0.26
WH	-1.30	-1.40	-7.34
XN	-1.12	-1.06	4.72
YC	-1.00	-1.20	-19.81
EZ	-1.59	-0.99	37.31
HG	-1.07	-1.08	-0.44
HS	-1.69	-1.49	11.74
YY	-0.61	-0.68	-12.44
CD	-0.66	-0.83	-24.93
CS	-0.84	-1.03	-23.03

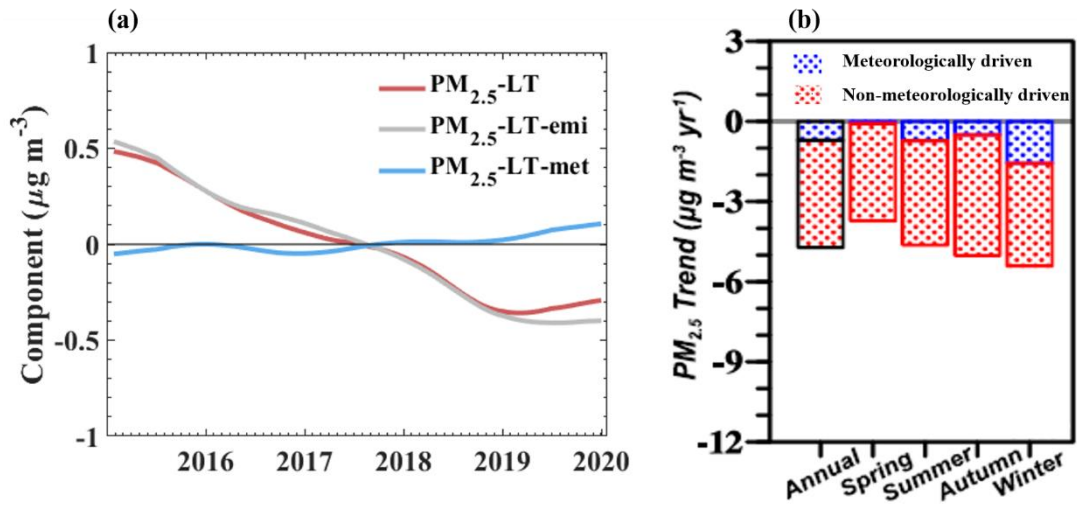


**Figure S1** (a) The regional averaged long-term (PM<sub>2.5</sub>-LT), emission-related long-term (PM<sub>2.5</sub>-LT-emi) and meteorology-related long-term (PM<sub>2.5</sub>-LT-met) components over the THB from 2015 to 2019. (b) Meteorologically driven, and non-meteorologically (emission) driven trends of annual and seasonal PM<sub>2.5</sub> concentrations during 2014–2018 for Central China. Blue and red bars respectively represent meteorologically driven trends and non-meteorologically (emission) driven trends (Chen et al., 2020).

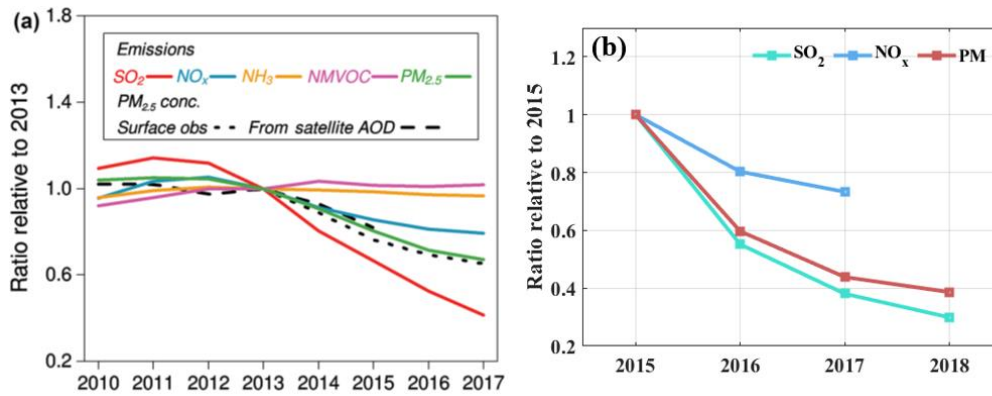


**Figure S2** (a) Interannual variations in the ratios of MEIC emissions for 2010–2017 compared with satellite- and ground-based observations relative to those in 2013 (Zheng et al., 2018), (b) interannual variations in the ratios of annual total emission of SO<sub>2</sub>, NO<sub>x</sub> and PM relative to those in 2015 averaged over the THB reported by National Bureau of Statistic of China.

### 1.1 Air pollutant emission inventories

For anthropogenic pollutant emissions, we used the monthly multi-resolution emission inventory for China (MEIC)

covering 2013–2017 (<http://www.meicmodel.org/>, last access: January 18, 2022), which was developed by Tsinghua University and has been evaluated by satellite remote sensing and ground based observations (Zheng et al., 2018). This inventory considers emissions of sulfur dioxide (SO<sub>2</sub>), nitrogen oxides (NO<sub>x</sub>), non-methane volatile organic compounds (NMVOCs), ammonia (NH<sub>3</sub>), carbon monoxide (CO), PM<sub>2.5</sub>, PM<sub>10</sub>, black carbon (BC), organic carbon (OC) and carbon dioxide (CO<sub>2</sub>) from power generation, industrial, residential, transportation and agricultural sectors, which has been used in modeling studies with a reliability (Gao et al., 2020; Liu et al., 2020). Considering the influence of primary emissions and gaseous precursors on PM<sub>2.5</sub>, we calculated the anthropogenic emissions of SO<sub>2</sub>, NO<sub>x</sub>, NH<sub>3</sub>, PM<sub>2.5</sub>, BC, OC and other species in 2018 and 2019 with quadratic function fitting based on the total emission of 2013–2017 from MEIC.

## **1.2 WRF-Chem modeling configuration**

The WRF-Chem version 3.9 was employed in this study with two nesting domains with horizontal resolutions of 81 km and 27 km cover Asian region and Eastern China (Fig. S3), with 33 vertical layers extending from the surface to 100 hPa. The physical parameterizations included the Noah land surface model, Grell 3D cumulus parameterization (Grell et al., 2005), the Mesoscale Model (MM5) similarity surface layer, the Yonsei University (YSU) boundary layer scheme (Hong and Noh, 2006), the Rapid Radiative Transfer Model (RRTM) longwave scheme (Mlawer et al., 1997), the Goddard shortwave scheme (Chou and Suarez, 1998) and the Lin microphysics scheme (Lin et al., 1983). The gas phase chemical mechanism CBMZ (Zaveri and Peters, 1999) coupled with the 4-bin sectional MOSAIC model with aqueous chemistry (Zaveri et al., 2008) was adopted. Initial and boundary meteorological conditions were driven with the reanalysis meteorological data in the horizontal resolutions of 1 °×1 ° obtained from NCEP (<https://rda.ucar.edu/datasets/ds083.2/>, last access: January 18, 2022).

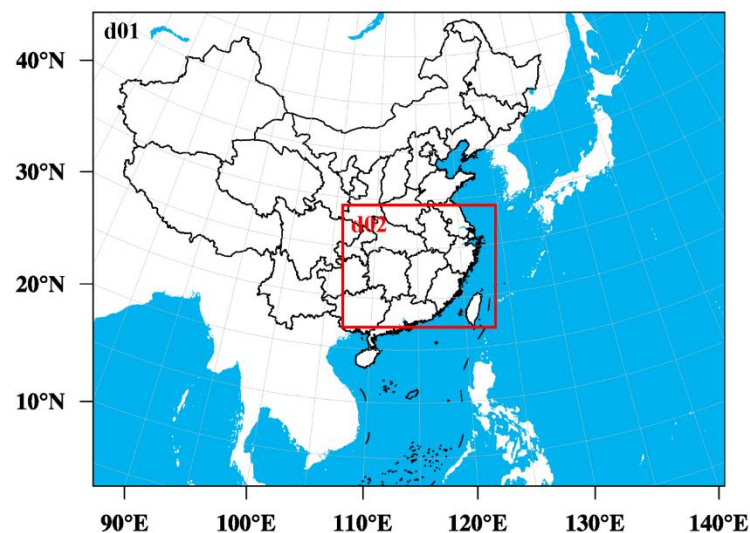


**Figure S3** Two nesting domains d01 and d02 for the WRF-Chem simulation.

### 1.3 Experiment design

To evaluate the effect of changes in meteorological conditions and anthropogenic emissions on  $PM_{2.5}$  variations, three sets of modeling experiments with WRF-Chem were designed for December from 2015 to 2019 (Table S6): (1) control tests (CTRL), simulations with changing meteorology and anthropogenic emissions over 2015–2019, (2) sensitivity tests on meteorology (SENS-MET), simulations with changing meteorological conditions and fixed anthropogenic emissions of 2015, and (3) sensitivity tests on emissions (SENS-EMI), simulations with changing anthropogenic emissions and fixed meteorological conditions of 2015.

**Table S6** Settings of WRF-Chem simulation experiments for modeling the effects of changes in meteorological conditions and anthropogenic emissions on  $PM_{2.5}$  variations

	Experiments	Descriptions
Control tests	M15E15	Model run with 2015 meteorology and 2015 emission
(CTRL)	M16E16	Model run with 2016 meteorology and 2016 emission

	M17E17	Model run with 2017 meteorology and 2017 emission
	M18E18	Model run with 2018 meteorology and 2018 emission
	M19E19	Model run with 2019 meteorology and 2019 emission
Sensitivity tests on	M16E15	Model run with 2016 meteorology and 2015 emission
meteorology	M17E15	Model run with 2017 meteorology and 2015 emission
(SENS-MET)	M18E15	Model run with 2018 meteorology and 2015 emission
	M19E15	Model run with 2019 meteorology and 2015 emission
Sensitivity tests on	M15E16	Model run with 2015 meteorology and 2016 emission
emissions	M15E17	Model run with 2015 meteorology and 2017 emission
(SENS-EMI)	M15E18	Model run with 2015 meteorology and 2018 emission
	M15E19	Model run with 2015 meteorology and 2019 emission

#### 1.4 Modeling verification

The WRF-Chem experiments CTRL simulated meteorological fields, which included relative humidity, wind speed, pressure and air temperature were compared with observations at 14 sites over the THB. The correlation coefficients were calculated and found to pass the significance level of 0.01, and the normalized standardized deviations were determined to be low (Taylor, 2001) (Fig. S4). Based on these results, it was evaluated that the WRF-Chem modeling meteorology was reasonably consistent with observations.

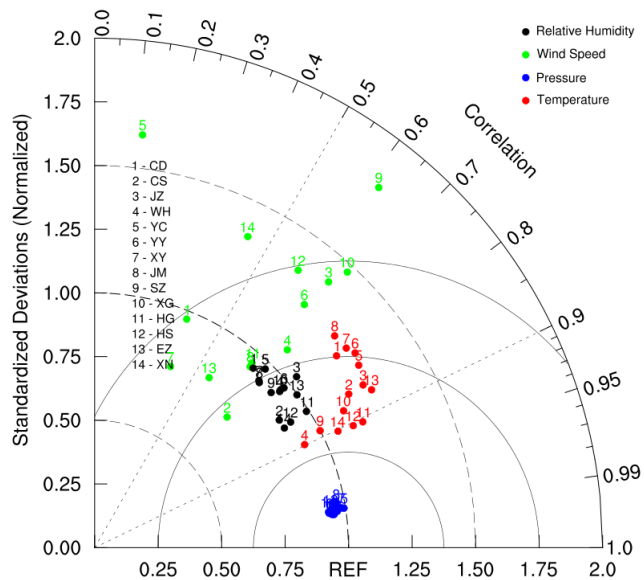


**Figure S4** A Taylor plot with the normalized standard deviations and correlation coefficients between WRF-Chem simulated and observed meteorological fields. The radian of the sector represents the correlation coefficient. The solid line indicates the ratio of standard deviation between simulations and observations. The distance from the marker to “REF” reflect the normalized root-mean-square error (NRMSE).

Figure S5 shows the daily variations of regional averaged  $PM_{2.5}$  concentrations over the 14 sites in THB for December of 2015–2019. The general variations of simulated  $PM_{2.5}$  concentrations were consistent with that of the observed  $PM_{2.5}$  concentrations. The evaluation results of regional averaged  $PM_{2.5}$  during five simulation periods for 14 sites in the THB were listed in Table S7. The simulated  $PM_{2.5}$  concentrations were slightly overestimated with NMBs and NMEs less than 40 % and 50 % respectively in 5 years. The values of NMBs and NMEs were comparable to other modelling studies (Zhang et al., 2019), fell within the “good” or “satisfactory” criteria (Boylan and Russell, 2006; Morris et al., 2005). The high correlation coefficients (over 0.50, passing the confidence level of 99 %) indicated the WRF-Chem simulation of experiments CTRL could reasonably reproduce the  $PM_{2.5}$  observations, which could be used in the further analysis of emission and meteorological impact on  $PM_{2.5}$  change.

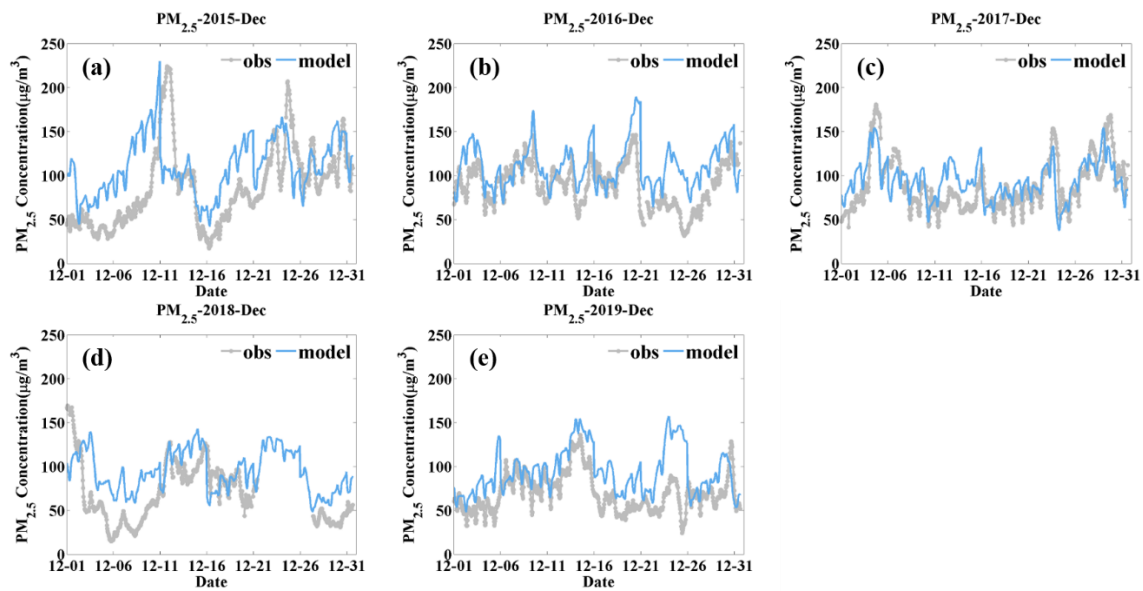


**Figure S5** Daily variations of observed (gray lines) and simulated (blue lines)  $PM_{2.5}$  averaged over the 14 sites in the THB for December of (a) 2015, (b) 2016, (c) 2017, (d) 2018, and (e) 2019.

**Table S7** Evaluation results for the modeling  $PM_{2.5}$  concentrations with the observations in December from 2015 to 2019. Obs. is mean observation; Sim. is mean simulation; r is correlation coefficient; RMSE is root mean square error; MFB is the mean fractional bias; MFE is the mean fractional error.

Year	Obs. ( $\mu\text{g m}^{-3}$ )	Sim. ( $\mu\text{g m}^{-3}$ )	r	RMSE	MFB(%)	MFE(%)
2015	85.69	109.86	0.46	47.74	31.90	43.44
2016	89.47	110.34	0.57	31.16	22.32	26.59
2017	87.54	93.80	0.63	23.84	8.69	22.17
2018	69.06	90.88	0.56	36.67	37.38	45.00
2019	68.70	93.35	0.52	34.34	31.03	33.61

**References:**

Boylan, J. W., and Russell, A. G.: PM and light extinction model performance metrics, goals, and criteria for three-dimensional air quality models, *Atmospheric environment*, 40, 4946-4959, 2006.

Chen, L., Zhu, J., Liao, H., Yang, Y., and Yue, X.: Meteorological influences on PM<sub>2.5</sub> and O<sub>3</sub> trends and associated health burden since China's clean air actions, *Sci Total Environ*, 744, 140837, 10.1016/j.scitotenv.2020.140837, 2020.

Chou, M. D., and Suarez, M. J.: Parameterizations for Cloud Overlapping and Shortwave Single-Scattering, *Journal of Climate*, 11, 1998.

Gao, M., Liu, Z., Zheng, B., Ji, D., Sherman, P., Song, S., Xin, J., Liu, C., Wang, Y., Zhang, Q., Xing, J., Jiang, J., Wang, Z., Carmichael, G. R., and McElroy, M. B.: China's emission control strategies have suppressed unfavorable influences of climate on wintertime PM<sub>2.5</sub> concentrations in Beijing since 2002, *Atmospheric Chemistry and Physics*, 20, 1497-1505, 10.5194/acp-20-1497-2020, 2020.

Grell, G. A., Peckham, S. E., Schmitz, R., McKeen, S. A., Frost, G., Skamarock, W. C., and Eder, B.: Fully coupled "online" chemistry within the WRF model, *Atmospheric Environment*, 39, 6957-6975, 10.1016/j.atmosenv.2005.04.027, 2005.

Hong, S. Y., and Noh, Y.: A New Vertical Diffusion Package with an Explicit Treatment of Entrainment Processes, *Monthly Weather Review*, 134, 2318-2341, 10.1175/mwr3199.1, 2006.

Lin, Y. L., Farley, R. D., and Orville, H. D.: Bulk Parameterization of the Snow Field in a Cloud Model, *Journal of Climate and Applied Meteorology*, 22, 1065-1092, 1983.

Liu, Q., Liu, D., Gao, Q., Tian, P., Wang, F., Zhao, D., Bi, K., Wu, Y., Ding, S., Hu, K., Zhang, J., Ding, D., and Zhao, C.: Vertical characteristics of aerosol hygroscopicity and impacts on optical properties over the North China Plain during winter, *Atmospheric Chemistry and Physics*, 20, 3931-3944, 10.5194/acp-20-3931-2020, 2020.

Mlawer, E. J., Taubman, S. J., Brown, P. D., Iacono, M. J., and Clough, S. A.: Radiative transfer for inhomogeneous atmospheres: RRTM, a validated correlated-k model for the longwave, *Journal of Geophysical Research: Atmospheres*, 102, 16663-16682, 10.1029/97jd00237, 1997.

Morris, R. E., McNally, D. E., Tesche, T. W., Tonnesen, G., Boylan, J. W., and Brewer, P.: Preliminary evaluation of the Community Multiscale Air Quality model for 2002 over the southeastern United States, *Journal of the Air & Waste Management Association*, 55, 1694-1708, 2005.

Taylor, K. E.: Summarizing multiple aspects of model performance in a single diagram, *Journal of Geophysical Research:*

Atmospheres, 106, 7183-7192, 10.1029/2000jd900719, 2001.

Zaveri, R. A., and Peters, L. K.: A new lumped structure photochemical mechanism for large-scale applications, *Journal of Geophysical Research: Atmospheres*, 104, 30387-30415, 10.1029/1999jd900876, 1999.

Zaveri, R. A., Easter, R. C., Fast, J. D., and Peters, L. K.: Model for Simulating Aerosol Interactions and Chemistry (MOSAIC), *Journal of Geophysical Research*, 113, 10.1029/2007jd008782, 2008.

Zhang, L., Guo, X., Zhao, T., Gong, S., Xu, X., Li, Y., Luo, L., Gui, K., Wang, H., Zheng, Y., and Yin, X.: A modelling study of the terrain effects on haze pollution in the Sichuan Basin, *Atmospheric Environment*, 196, 77-85, 10.1016/j.atmosenv.2018.10.007, 2019.

Zheng, B., Tong, D., Li, M., Liu, F., Hong, C. P., Geng, G. N., Li, H. Y., Li, X., Peng, L. Q., and Qi, J.: Trends in China's anthropogenic emissions since 2010 as the consequence of clean air actions, *Atmospheric Chemistry and Physics*, 18, 14095-14111, 2018.